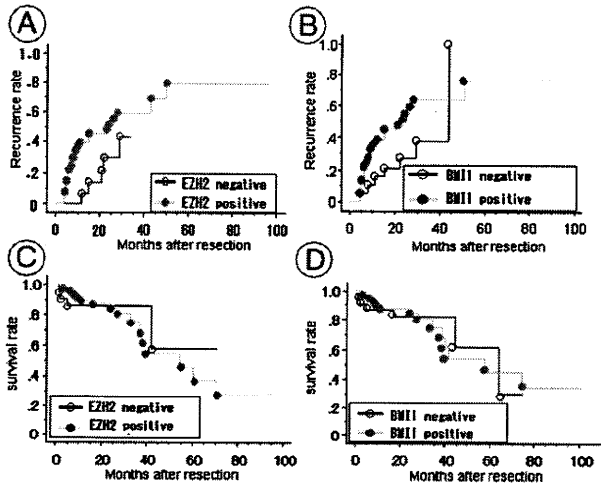

Fig. 4 Kaplan-Meier curves for the prognostic analyses. A and B, Cumulative recurrence rate with regard to EZH2 expression (A) and BMI1 expression (B). C and D, Cumulative survival rate with regard to EZH2 expression (C) and BMI1 expression (D).

The potential risk factors affecting tumor recurrence were analyzed by univariate Cox proportional hazards regression, and variables of P value less than 0.1 (the presence of BMI1, risk ratio, 2.3, $P = .053$; the presence of EZH2, risk ratio, 2.5, $P = .060$; age ≤65 years, risk ratio, 2.4, $P = .018$; AFP >40 mg/mL, risk ratio, 2.5, $P = .013$; albumin ≤3.8 mg/dL, risk ratio, 2.3, $P = .020$; the presence of portal vein invasion, risk ratio, 2.1, $P = .050$; TNM stage I + II, risk ratio, 0.40, $P = .015$) were further studied by multivariate analysis. However, we found that no variables examined in this multivariate analysis showed a statistically significant correlation with recurrence (the presence of BMI1, risk ratio, 1.4, $P = .51$; the presence of EZH2, risk ratio, 1.6, $P = .47$; age ≤65 years, risk ratio, 2.4, risk ratio, 2.0, $P = .07$; AFP >40 mg/mL, risk ratio, 2.0, $P = .12$; albumin ≤3.8 mg/dL, risk ratio, 2.2, $P = .11$; the presence of portal vein invasion, risk ratio, 0.64, $P = .43$; TNM stage I + II, risk ratio, 0.52, $P = .10$).

We found no effect on survival and recurrence in tumors that simultaneously expressed both EZH2 and BMI1 as compared with those that expressed only one of these proteins ($P = .61$ for recurrence and $P = .58$ for survival, as determined by Kaplan-Meier analysis).

4. Discussion

Hepatocellular carcinoma is one of the most common malignancies, and chronic viral infection by hepatitis B or C virus is well recognized as a major risk factor [17]. Therapeutic advancements such as nucleotide analogues and interferon has successfully improved hepatitis viremia and reduced the incidence of hepatocellular carcinoma, but the mortality rate of hepatocellular carcinoma remains high in spite of recent advances in cancer therapy [18]. In hepatocarcinogenesis, it appears that repeated injury and regeneration of damaged liver cells induce genetic and epigenetic dysregulation, which ultimately contribute to cancer development [19,20]. Recent studies highlight the pivotal role of polycomb group proteins in cancer [1]. However, our knowledge on their implications in hepatocarcinogenesis remains limited [21].

At first, we examined the growth activity of HepG2 cells in loss-of-function assays. The MTS assays showed that EZH2 or BMI1 knockdown mediated significant cell growth inhibition. This finding appears to be consistent with previous observations suggesting a role for EZH2 or BMI1 in a variety of immortalized and transformed cells [6,7,22]. Interestingly, knockdown of both EZH2 and BMI1 augmented cell growth inhibition, which indicated that the function of EZH2 might partly differ from that of BMI1 in molecular mechanisms underlying proliferation of hepatocellular carcinoma cells.

On the other hand, immunohistochemical analyses showed that increased expression of either EZH2 or BMI1 protein was observed in 60 (69.8%) of 86 hepatocellular carcinoma samples. Meanwhile, only 5.8% and 4.7% of surrounding nontumor tissues expressed EZH2 and BMI1, respectively. These results unveil preferential up-regulation of polycomb group protein expression during hepatocarcinogenesis and might implicate a special role for polycomb group proteins in the development and progression of hepatocellular carcinoma. Given that EZH2 and BMI1 were frequently coexpressed in the same samples, there might be functional crosstalk between EZH2 and BMI1 in the pathogenesis of hepatocellular carcinoma. Conversely, 26 (30.2%) of 86 samples exhibited expression of neither protein, which might be reflective of inherent heterogeneity with respect to origin of hepatocellular carcinoma and/or underlying molecular mechanisms.

Analyses of EZH2 mRNA expression in hepatocellular carcinoma samples based on real-time reverse transcriptase polymerase chain reaction have previously documented no significant correlation between EZH2 expression and disease-free survival [21]. Recently, another group reported that overexpression of EZH2 and BMI1 is associated with aggressive biologic behavior including vascular invasion and lymph node metastasis [23,24]. To examine whether protein expression of EZH2 and BMI1 are good biomarkers for recurrence and survival in our samples, we conducted prognostic analyses. The present analyses demonstrate that increased expression of both EZH2 and BMI1 proteins significantly correlated with recurrence after hepatectomy ($P = .029$ and $P = .039$, respectively), although there was no significant correlation between the expression of these polycomb group proteins and survival. Analyses of clinicopathologic parameters showed lower levels of serum albumin and advanced stage of TNM in EZH2-positive patients compared with EZH2-negative patients, which might indicate advanced liver dysfunction and tumor stage in EZH2-positive patients. In contrast, the significant

correlation between high EZH2 expression and portal vein invasion of the tumor, which was previously reported by mRNA expression-based analyses [21], was not detected in this study ($P = .23$).

In conclusion, our studies showed that polycomb proteins, in particular, EZH2 and BMI1, can have a strong effect on proliferation of hepatocellular carcinoma cells and that simultaneous knockdown of EZH2 and BMI1 has more marked effect on cell growth inhibition than knockdown of either protein alone. Immunohistochemical analyses further demonstrated a clear association between EZH2 and BMI1 expression and the development and progression of hepatocellular carcinoma, as well as recurrence after curative surgery. Thus, EZH2 and BMI1 could be target molecules in the development of new treatment strategies against hepatocellular carcinoma.

Acknowledgments

The authors thank Dr Huroyuki Miyoshi (RIKEN, Tsukuba, Japan) for providing lentiviral vectors and Dr Yoh Zen (Kanazawa University, Kanazawa, Japan) for technical assistance in immunohistochemical analyses.

References

[1] Valk-Lingbeek ME, Bruggeman SWM, van Lohuizen M. Stem cells and cancer: the polycomb connection. Cell 2004;118:409-18.

[2] Sparmann A, van Lohuizen M. Polycomb silencers control cell fate, development and cancer. Nat Rev Cancer 2006;6:846-56.

[3] Iwama A, Oguro H, Negishi M, et al. Enhanced self-renewal of hematopoietic stem cells mediated by the polycomb gene product, Bmi-1. Immunity 2004;21:843-51.

[4] Gil J, Peters G. Regulation of the INK4b-ARF-INK4a tumour suppressor locus: all for one or one for all. Nat Rev Mol Cell Biol 2006;7:667-77.

[5] Oguro H, Iwama A, Morita Y, Kamijo T, van Lohuizen M, Nakauchi H. Differential impact of Ink4a and Arf on hematopoietic stem cells and their bone marrow microenvironment in Bmi1-deficient mice. J Exp Med 2006;203:2247-53.

[6] Visser HP, Gunster MJ, Kluin-Nelemans HC, et al. The Polycomb group protein EZH2 is upregulated in proliferating, cultured human mantle cell lymphoma. Br J Haematol 2001;112:950-8.

[7] Croonquist PA, Van Ness B. The polycomb group protein enhancer of zeste homolog 2 (*EZH2*) is an oncogene that influences myeloma cell growth and the mutant ras phenotype. Oncogene 2005;24:6269-80.

[8] van Lohuizen M, Verbeek S, Scheijen B, Wientjens E, van der Gulden H, Berns A. Identification of cooperating oncogenes in Eμ-myc transgenic mice by provirus tagging. Cell 1991;65:737-52.

[9] Smith KS, Chanda SK, Lingbeek M, et al. Bmi-1 regulation of INK4A-ARF is a downstream requirement for transformation of hematopoietic progenitors by E2a-Pbx1. Mol Cell 2003;12:393-400.

[10] Mohty M, Yong AS, Szydlo RM, Apperley JF, Melo JV. The polycomb group BMI1 gene is a molecular marker for predicting prognosis of chronic myeloid leukemia. Blood 2007;110:380-3.

[11] Chowdhury M, Mihara K, Yasunaga S, Ohtaki M, Takihara Y, Kimura A. Expression of Polycomb-group (PcG) protein BMI-1 predicts prognosis in patients with acute myeloid leukemia. Leukemia 2007;21:1116-22.

[12] van Kemenade FJ, Raaphorst FM, Blokzijl T, et al. Coexpression of BMI-1 and EZH2 polycomb-group proteins is associated with cycling cells and degree of malignancy in B-cell non–Hodgkin lymphoma. Blood 2001;97:3896-901.

[13] Varambally S, Dhanasekaran SM, Zhou M, et al. The polycomb group protein EZH2 is involved in progression of prostate cancer. Nature 2002;419:624-9.

[14] Kleer CG, Cao Q, Varambally S, et al. EZH2 is a marker of aggressive breast cancer and promotes neoplastic transformation of breast epithelial cells. Proc Natl Acad Sci U S A 2003;100:11606-11.

[15] Kim JH, Yoon SY, Jeong SH, et al. Overexpression of Bmi-1 oncoprotein correlates with axillary lymph node metastases in invasive ductal breast cancer. Breast 2004;13:383-8.

[16] Liver Cancer Study Group of Japan. The general rules for the clinical and pathological study of primary liver cancer. 2nd English ed. Tokyo: Kanehara & Co., Ltd.; 2003.

[17] Wang BE, Ma WM, Sulaiman A, et al. Demographic, clinical, and virological characteristics of hepatocellular carcinoma in Asia: survey of 414 patients from four countries. J Med Virol 2002;67:394-400.

[18] Colombo M, Donato MF. Prevention of hepatocellular carcinoma. Semin Liver Dis 2005;25:155-61.

[19] Bruix J, Boix L, Sala M, Llovet JM. Focus on hepatocellular carcinoma. Cancer Cell 2004;5:215-9.

[20] Roberts LR, Gores GJ. Hepatocellular carcinoma: molecular pathways and new therapeutic targets. Semin Liver Dis 2005;25:212-25.

[21] Sudo T, Utsunomiya T, Mimori K, et al. Clinicopathological significance of EZH2 mRNA expression in patients with hepatocellular carcinoma. Br J Cancer 2005;92:1754-8.

[22] Chen Y, Lin MC, Yao H, et al. Lentivirus-mediated RNA interference targeting enhancer of zeste homolog 2 inhibits hepatocellular carcinoma growth through down-regulation of stathmin. Hepatology 2007;46:200-8.

[23] Sasaki M, Ikeda H, Itatsu K, et al. The overexpression of polycomb group proteins Bmi1 and EZH2 is associated with the progression and aggressive biological behavior of hepatocellular carcinoma. Lab Invest 2008;00 00:1-10.

[24] Sasaki M, Yamaguchi J, Itatsu K, Ikeda H Nakanuma Y. Over-expression of polycomb group protein EZH2 relates to decreased expression of $P16^{INK4a}$ in cholangiocarcinogenesis in hepatolithiasis. J Pathol 2008;215:175-83.

Liver International ISSN 1478-3223

CLINICAL STUDIES

Phylogenetic analysis of hepatitis A virus in sera from patients with hepatitis A of various severities

Keiichi Fujiwara[1], Hiroshige Kojima[1], Yutaka Yonemitsu[1], Shin Yasui[1], Fumio Imazeki[1], Makoto Miki[2], Kazuyuki Suzuki[3], Isao Sakaida[4], Kiwamu Okita[4], Eiji Tanaka[5], Masao Omata[6] and Osamu Yokosuka[1]

1 Department of Medicine and Clinical Oncology, Graduate School of Medicine, Chiba University, Chiba, Japan
2 Department of Internal Medicine, Yokohama Higashi National Hospital, Kanagawa, Japan
3 First Department of Internal Medicine, Iwate Medical University, Iwate, Japan
4 Department of Gastroenterology and Hepatology, Yamaguchi University School of Medicine, Yamaguchi, Japan
5 Department of Medicine, Shinshu University School of Medicine, Nagano, Japan
6 Department of Gastroenterology, Faculty of Medicine, University of Tokyo, Tokyo, Japan

Keywords
2B – 2C – 5′NTR – fulminant hepatitis – hepatitis A – hepatitis A virus

Abbreviations
AH, acute hepatitis; AHs, acute hepatitis severe type; FH, fulminant hepatitis; HAV, hepatitis A virus; PT, prothrombin time.

Correspondence
Keiichi Fujiwara, MD, PhD, Department of Medicine and Clinical Oncology, Graduate School of Medicine, Chiba University, 1-8-1 Inohana, Chuo-ku, Chiba 260-8670, Japan
Tel: +81 43 226 2083
Fax: +81 43 226 2088
e-mail: fujiwara-cib@umin.ac.jp

Received 13 August 2008
Accepted 4 October 2008

DOI:10.1111/j.1478-3231.2008.01919.x

Abstract

Background: We analysed the association of the 5′ nontranslated region (5′NTR), nonstructural proteins 2B and 2C of the hepatitis A virus (HAV) genome, whose mutations have previously been shown to be important for enhanced replication in cell culture systems, in order to align all our data and examine whether genomic differences in HAV are responsible for the range of clinical severities. *Methods:* Our accumulated HAV strains of 5′NTR [nucleotide(nt) 200 and 500], entire 2B and 2C from 25 Japanese patients with sporadic hepatitis A, consisting of seven patients with fulminant hepatitis (FH), five with severe acute hepatitis (AHs) and 13 with self-limited acute hepatitis (AH), in whom the sequences of all three regions were available, were subjected to phylogenetic analysis. *Results:* Fulminant hepatitis patients had fewer nucleotide substitutions in 5′NTR, had a tendency to have more amino acid (aa) substitutions in 2B and had fewer aa substitutions in 2C than AH patients. Four FH and two AHs with a higher viral replication were located in the near parts of the phylogenetic trees, indicating the association between the severity of hepatitis A and genomic variations in 5′NTR, 2B and 2C of HAV. *Conclusions:* Our study suggests that genetic variations in HAV not in one specific region but in 5′NTR, 2B and 2C might cooperatively influence replication of the virus, and thereby affect virulence. Viral factors should be considered and examined when discussing the mechanisms responsible for the severity of hepatitis A.

Hepatitis A is still a major problem worldwide, not only in underdeveloped countries but also in industrialized nations. Because of improvements in sanitation, there have been no hepatitis A epidemics in Japan in recent years. However, sporadic cases of hepatitis A have not been rare of late. Although the majority of hepatitis A cases are self-limited acute hepatitis (AH), some develop into severe forms of hepatitis (1). In fact, in the past several years, there has been an increase in the numbers of patients with sporadic hepatitis A, especially the more severe kind, visiting our hospital. Our analysis of the possible factors responsible for the disease severity in our patients revealed no significant differences in terms of background including age, suggesting that viral factors might be involved in determining the severity of the disease (2, 3).

Hepatitis A virus (HAV) is the sole member of the hepatovirus genus and a member of the Picornavirus family. Virological studies have revealed that HAV is a positive-strand RNA virus comprising approximately 7500 nucleotides and containing a 5′ nontranslated region (NTR), a single long open reading frame encoding a large polyprotein and a 3′NTR. A large polyprotein is cleaved by the viral protease to produce the P1, P2 and P3 regions. The P1 region encodes four structural proteins – VP4, VP2, VP3 and VP1. The P2 and P3 regions encode nonstructural proteins 2A, 2B and 2C, and 3A, 3B, 3C and 3D respectively (4). As far as is known, nonstructural protein 2A participates in virion morphogenesis (5). 2B and 2C play important roles in the replication of viral RNA. 2C is a multifunctional protein and is considered to have helicase and NTPase activities. 2C or 2BC have membrane- and RNA-binding properties (6). 3B is considered to be a genome-linked viral protein (Vpg), 3A a pre-Vpg, 3C a viral protease and 3D an RNA-dependent RNA polymerase.

It was reported that the strains adapted to cell culture systems have mutations in 5′NTR and the P2 region of HAV (7, 8). Zhang *et al.* (9) reported that rapidly replicating, cytopathic variants of HAV isolated from cultured cells required mutations within 5′NTR, 2B and 2C, and these mutations acted cooperatively. Raychaudhuri *et al.* (10) reported that the simian virus 2C gene could confer the phenotype of virulence to an otherwise attenuated virus, and clusters of residues near both ends of the 2C protein were required for virulence using chimeras between human and simian strains of hepatitis A virus in tamarins.

Despite advances in the understanding of HAV, a correlation between the HAV genome and the clinical status of hepatitis A has not been established. Durst *et al.* (11) reported a cluster of fulminant hepatitis A, in which the severity of the infection in three siblings was related to the virulence of HAV. To examine the possibility of differences in hepatitis A viruses in terms of the different categories of hepatitis, we have analysed the viral genomes in sera from hepatitis A patients with a variety of clinicopathological features and reported the associations between some viral regions and clinical severities (3, 12–18).

When analysing the viral genome, rather than focusing on one specific region, perhaps several portions of the HAV genome should be investigated. In the present study, we examined the clinicopathological features of hepatitis A and possible correlations with variations in the three regions of 5′NTR, 2B and 2C of the HAV genome, whose mutations have previously been shown to be important for enhanced replication and virulence in cell culture systems and simians, in the same patients using phylogenetic analysis.

Materials and methods

Patients

Serum samples from 25 patients with hepatitis A in Japan were collected between 1986 and 1999 and stored at −20 °C until analysis. Informed consent was obtained from the patients or appropriate family members. These patients were diagnosed based on the positivity of the IgM antibody to HAV (IgM anti-HAV) in conjunction with compatible symptoms and laboratory findings.

Among the patients seven had fulminant hepatitis (FH), five had severe acute hepatitis (AHs) and 13 had self-limited AH. Patients with a prothrombin time < 40% of control were defined as AHs, and those with hepatic encephalopathy as FH. Patients with significant increases in serum blood urea nitrogen and creatinine (more than three times the upper level of the normal range) were judged to be undergoing acute renal failure. The patients were also investigated for histories of recent exposure to drugs and chemical agents as well as heavy alcohol consumption (> 50 g/day for > 5 years).

None of the patients had clinical or laboratory evidence of acquired immune deficiency syndrome.

Serological markers

IgM antibody to HBc(IgM anti-HBc), HBsAg and second-generation antibody to hepatitis C virus (HCV) were examined in all cases. IgM anti-HAV, IgM anti-HBc and HBsAg were measured by commercial radioimmunoassay kits (Abbott Laboratories, Chicago, IL, USA); second-generation HCV antibody was measured by the enzyme immunoassay kit (Ortho Diagnostics, Tokyo, Japan). In the FH and AHs patients, HCV RNA, IgM antibody to Epstein–Barr virus (IgM anti-EBV), IgM antibody to herpes simplex virus (IgM anti-HSV), IgM antibody to cytomegalovirus (IgM anti-CMV), anti-smooth muscle antibody, liver kidney microsomal antibody-1 and anti-mitochondrial antibody were also examined. HCV RNA was measured by nested reverse transcriptase-polymerase chain reaction (RT-PCR) as described by the authors (19). IgM anti-EBV, IgM anti-CMV and IgM anti-HSV were examined by enzyme-linked immunosorbent assays. Anti-nuclear antibody, anti-smooth muscle antibody, anti-mitochondrial antibody and anti-liver kidney microsomal-1 antibody were examined by the fluorescent antibody method.

Quantification of hepatitis A virus RNA by real-time reverse transcriptase-polymerase chain reaction

Serum viral RNA was extracted by the High Pure Viral RNA Kit (Roche Diagnostics GmbH, Mannheim, Germany). RT-PCR was carried out with a Hepatitis A Virus Quantification Kit (Roche Diagnostics) according to the manufacturer's instructions. Twenty microliters of the PCR mixture contained 15 μl of master mix from the kit and 5 μl of template RNA. The standards of HAV RNA are supplied with this kit. All reactions were performed in a LightCycler (Roche Diagnostics). The C_T values from clinical samples were plotted on the standard curve, and the number of copies wes calculated automatically. This method has a dynamic range of HAV RNA quantification between 0.5 and 5×10^6 copies/μl.

Amplification of serum hepatitis A virus RNA and direct sequencing

Hepatitis A virus RNA was examined by nested RT-PCR and direct sequencing as described previously (14, 17, 18).

Nucleotide sequence accession numbers

The nucleotide sequence data reported herein appear in DDBJ/EMBL/GenBank nucleotide sequence databases with the following accession numbers:

5′NTR

AB045327 for A1, AB045336 for A5, AB045330 for A204, AB045331 for A205, AB045332 for A206, AB045334 for A414, AB045338 for A601, AB045342 for A159, AB045344 for A160, AB045345 for A161, AB045350 for A302, AB045353 for A811, AB045672 for A7, AB045692

for A9, AB045568 for A20, AB045671 for A68, AB045680 for A75, AB045681 for A77, AB045366 for A162, AB045572 for A303, AB045646 for A304, AB045648 for A306, AB045649 for A307, AB045678 for A712 and AB045679 for A713.

2B

AB047652 for A1, AB047671 for A5, AB047660 for A204, AB047661 for A205, AB047662 for A206, AB047669 for A414, AB047673 for A601, AB047654 for A159, AB047655 for A160, AB047656 for A161, AB047663 for A302, AB047680 for A811, AB047675 for A7, AB047681 for A9, AB047658 for A20, AB047674 for A68, AB047678 for A75, AB047679 for A77, AB047657 for A162, AB047664 for A303, AB047665 for A304, AB047666 for A306, AB047667 for A307, AB047676 for A712 and AB047677 for A713.

2C

AB082174 for A1, AB082130 for A5, AB0821323 for A204, AB082133 for A205, AB082134 for A206, A082135 for A414, AB082137 for A601, AB082139 for A159, AB082140 for A160, AB082141 for A161, AB082145 for A302, AB082147 for A811, AB082148 for A7, AB082149 for A9, AB082150 for A20, AB082154 for A68, AB082155 for A75, AB082156 for A77, AB082160 for A162, AB082165 for A303, AB082166 for A304, AB082167 for A306, AB082168 for A307, AB082171 for A712 and AB082172 for A713.

Phylogenetic analysis

To determine the heterogeneity of the viral sequences obtained from the 25 patients, a phylogenetic tree was constructed by the neighbour-joining method. To confirm the reliability of the phylogenetic tree, bootstrap resampling tests were performed 1000 times. These analyses were conducted using a computer program, GENETYX-MAC version 10.1 (Software Development, Tokyo, Japan).

Statistical analysis

Differences in proportions among the groups were compared by Fisher's exact probability test, Student's *t*-test and Welch's *t*-test (DA STATS version 1.0, Nagata O, Tokyo, Japan).

Results

Clinicopathological characteristics of the patients

The characteristics of the 25 patients with hepatitis A analysed for HAV 5′NTR, 2B and 2C at admission are summarized in Table 1. None of the cases was associated with an epidemic.

Differences in the mean age, sex and presence of chronic liver disease among FH, AHs and AH, and between FH+AHs and AH, were not statistically significant. Serum was sampled 2–17 days after clinical onset. The mean ALT level was higher in AHs than that in AH ($P = 0.002$), and in FH+AHs than that in AH ($P = 0.003$). The mean prothrombin time was prolonged in FH compared with AHs ($P = 0.002$), FH compared with AH ($P < 0.001$), AHs compared with AH ($P < 0.001$) and FH+AHs compared with AH ($P < 0.001$). The mean total bilirubin level was higher in FH than that in AHs ($P = 0.049$).

Table 1. Characteristics of patients

	FH	AHs	AH
n	7	5	13
CLD	1†	1†	3†
Recovery/death	3/4‡	5/0‡	13/0‡
Sex (M/F)	3/4†	5/0†	7/6†
Age*	44.1 ± 13.5†	36.8 ± 12.9†	39.5 ± 9.1†
PT (%)*	16 ± 7§	34 ± 8§	63 ± 20§
ALT (IU/L)*	6337 ± 3838¶	6165 ± 1718¶	2873 ± 1733¶
T-Bil (mg/dl)*	9.4 ± 7.6‖	2.3 ± 0.8‖	5.0 ± 2.3‖

*Mean ± SD.

†Statistically not significant.

‡Statistically significant between FH and AH ($P = 0.007$) by Fisher's exact probability test.

§Statistically significant between FH and AHs ($P = 0.002$) by Student's *t*-test, FH and AH ($P < 0.001$) by Welch's *t*-test, and AHs and AH ($P < 0.001$) by Welch's *t*-test.

¶Statistically significant between AHs and AH ($P = 0.002$) by Student's *t*-test.

‖Statistically significant between AHs and FH ($P = 0.049$) and AHs and AH ($P = 0.002$) by Welch's *t*-test.

AH, acute hepatitis; AHs, severe acute hepatitis; ALT, alanine aminotransferase; CLD, chronic liver disease; FH, fulminant hepatitis; PT, prothrombin time; T-Bil, total bilirubin.

Four of seven patients with FH died of hepatic failure, and all patients with AHs and AH recovered ($P = 0.007$). All seven FH cases needed artificial liver support (plasma exchange and haemodiafiltration). Four (16%) patients – two (28%) with FH and two (15%) with AH – had acute renal failure and were treated by haemodiafiltration.

Two patients with AH were positive for HBsAg and antibody to HBe, and one patient with AH was positive for anti-nuclear antibody, but they showed a typical hepatitis A course. IgM anti-EBV, IgM anti-HSV, IgM anti-CMV, anti-nuclear antibody, anti-smooth muscle antibody, liver kidney microsomal antibody-1 and anti-mitochondrial antibody were negative in all examined cases of FH and AHs. One FH patient and one AHs patient had histories of heavy alcohol consumption. One male patient with AH was homosexual.

Histological examination was performed in all seven FH cases, two of five AHs cases and seven of 13 AH cases in the convalescent phase or postmortem. In the FH cases, liver histology revealed massive necrosis in three patients and submassive necrosis in one. Liver histology in the two patients with histories of heavy alcohol consumption showed pericellular fibrosis, consistent with alcoholic liver disease. The histological findings of the other cases showed AH to be in a residual phase or subsiding.

Phylogenetic analysis

The results of phylogenetic analysis are shown in Figures 1 and 2. Four FH (A204, A601, A414 and A1) and two AHs (A160 and A159) were located in the near parts of the phylogenetic trees (Fig. 2).

The clinical backgrounds, and the biochemical and viral characteristics are shown in Table 2. As described above, none of them were associated with an epidemic. Two of the FH patients died and the others recovered. HAV RNA was quantified by real-time RT-PCR in five of these six patients. Our other recent study of HAV RNA quantification revealed that the mean viral load in > 60 AH at admission was 2.75 ± 1.55 log copies/ml (20), and so these five patients had comparatively higher viral loads (4.35 ± 0.81 log copies/ml) ($P = 0.03$). The HAV genotype was IA in all patients, similar to the majority of Japanese patients in general.

Discussion

Although the severity of hepatitis A varies, it is not clear why it is more severe in some patients than that in others. It is thought that disease severity may be dependent on certain characteristics of the individual patients. It has been reported that ageing and underlying chronic liver disease could be factors that increase hepatitis A severity (21). Vento *et al.* (22) reported that patients with chronic hepatitis C had a substantial risk of FH and death associated with HAV superinfection.

During an urban epidemic in the US, it was described that hepatitis A caused serious illness and death and that complications were more frequent in patients 40 years of age and older, but that young healthy persons were also at risk for severe complications (23). A cluster of fulminant hepatitis A was reported, relating the severity of the infection in three siblings to the virulence of HAV, as the patients were all healthy before the infection and their illness followed a similar course (11).

In the past several years, increasing numbers of patients with sporadic hepatitis A, especially the more severe forms, have visited our hospital, but our analysis of factors possibly contributing to the severity of the disease failed to reveal any significant differences in patient characteristics including age (2, 3), suggesting that viral factors might determine the severity of the disease. To identify possible differences in hepatitis A viruses for different types of hepatitis, we analysed the HAV genome in sera from hepatitis A patients with various clinicopathological features. Our analysis of whole HAV genomes from three cases of FH and three cases of AH indicated possible associations between the severity of hepatitis A and the nucleotide substitutions in 5′NTR and the amino acid (aa) substitutions in 2B, although there were no unique nucleotide or aa substitutions. On the other hand, it was reported that mutations in 5′NTR, 2B and 2C of HAV were associated with cytopathic variants in cultured cells, and virulence in tamarins, as described above (9, 10). These various observations led us to analyse these three regions of HAV in greater numbers of clinical samples (14, 17, 18).

In our analysis of 5′NTR, FH and AHs patients had fewer nucleotide substitutions than AH in the central part of 5′NTR ($P < 0.001$) (14). Several regions of 5′NTR, including the pyrimidine-rich tract and internal ribosomal entry site, have been examined for possible correlations with replication of HAV RNA *in vitro*, and it has been reported that HAV strains adapted to cell culture systems have mutations in 5′NTR and the P2 region (8), and mutations in 5′NTR significantly enhanced growth of the virus in a cell culture system (24). Thus, nucleotide variations in 5′NTR may influence replication of the virus and thereby affect virulence.

In 2B, there seemed to be more mutations in the strains obtained from FH and AHs patients than in those obtained from AH patients in the central part (18). On the basis of cell culture studies, substitutions in the sequence of 2B protein have been suggested to be associated with the replication capability of the virus. One nucleotide substitution at nt 3889 in 2B, which changed Ala to Val in 2B-216, is responsible for differences in the growth rate of the virus along with the nucleotide substitutions in 2C and/or 5′NTR (25, 26). A substitution at the same nt 3889 appeared from the early stage of replication enhancement in cultured cells, and several HAV strains showed a cytopathic effect (8). An Ala-to-Val substitution in 2B-216 was not observed in our study.

In 2C, FH patients had fewer aa substitutions than AH patients ($P < 0.05$) (17). This indicates that viruses with fewer aa substitutions in 2C may be more virulent in comparison with strains with more aa substitutions. 2C is a multifunctional protein and is involved in replication of the viral genome. Analysis of the primary aa sequence of 2C shows homology with a family of proteins that contains a nucleoside triphosphate (NTP)-binding motif. This motif consists of elements 'A' and 'B'. The residues mutated within the conserved A and B sites of the NTP-binding motif are critical in RNA replication and virus proliferation (27). Elements A and B were conserved in all patients except one of FH. 2C is also suggested to be involved in the rearrangement of cellular membranes (28). The simian HAV 2C gene was reported to be required for virulence in tamarins (10). Thus, subtle substitutions in 2C might influence the replication capability of the virus and thereby affect virulence. We could not find specific nucleotide or aa substitutions in any of the regions.

In the present study, patients with FH had fewer nt substitutions in 5′NTR, and had a tendency to have more aa substitutions in 2B, and fewer aa substitutions in 2C, than patients with AH, and four FH and two AHs were located in the near parts of the phylogenetic trees, indicating the association between severity of hepatitis A and genomic variations in 5′NTR, 2B and 2C of HAV. In these patients, HAV load was higher than that of AH

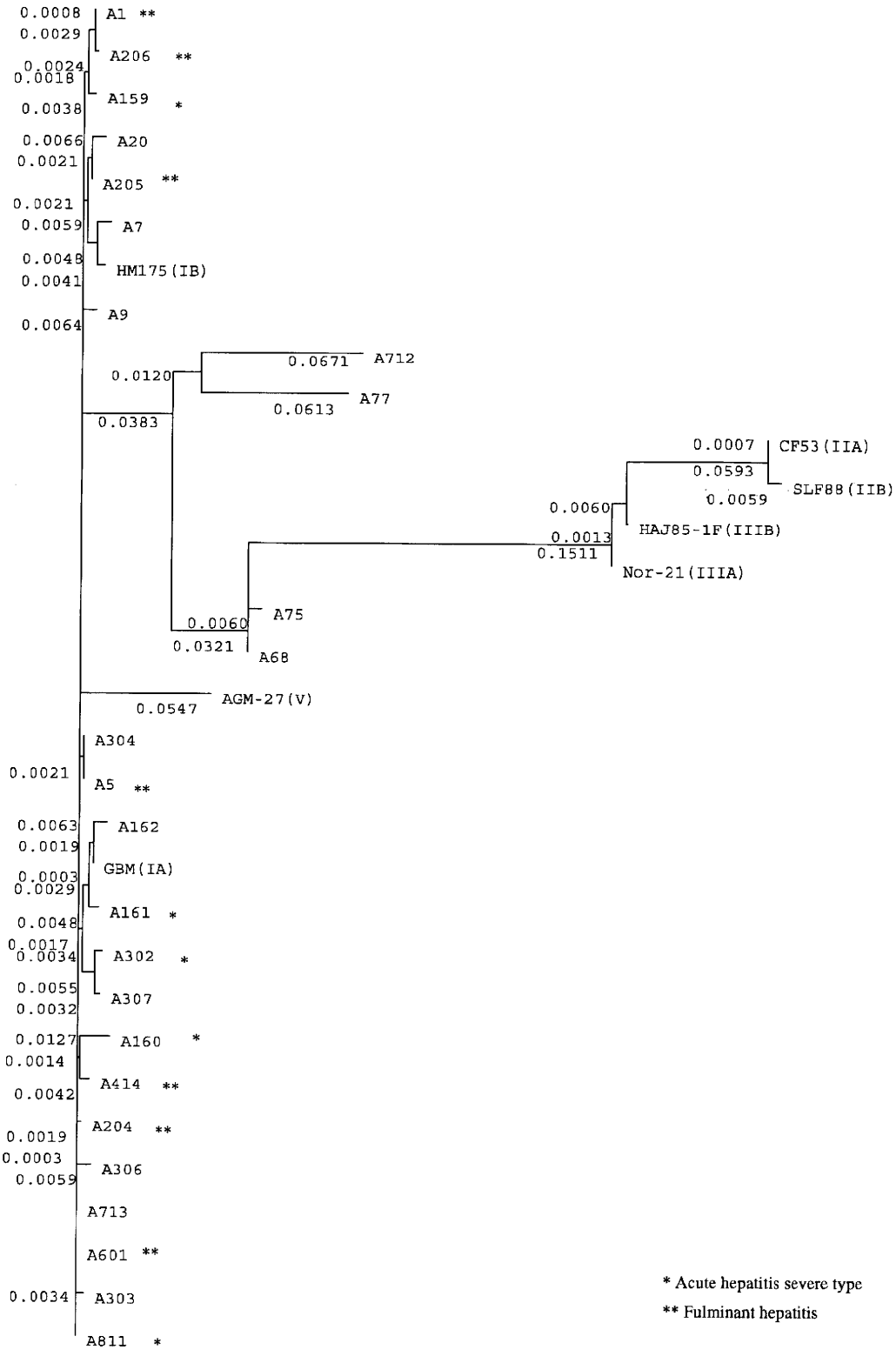

Fig. 1. Genetic relatedness between individual hepatitis A virus (HAV) strains between nucleotides 200 and 500 of the 5′ nontranslated region recovered from 25 patients and HAV reference strains GBM (subgenotype IA), HM175 (subgenotype IB), CF53 (subgenotype IIA), SLF88 (subgenotype IIB), Nor-21 (subgenotype IIIA), HAJ85-1F (subgenotype IIIB) and AGM27 (genotype V). Numbers beside the phylogenetic roots are the results of bootstrap analyses.

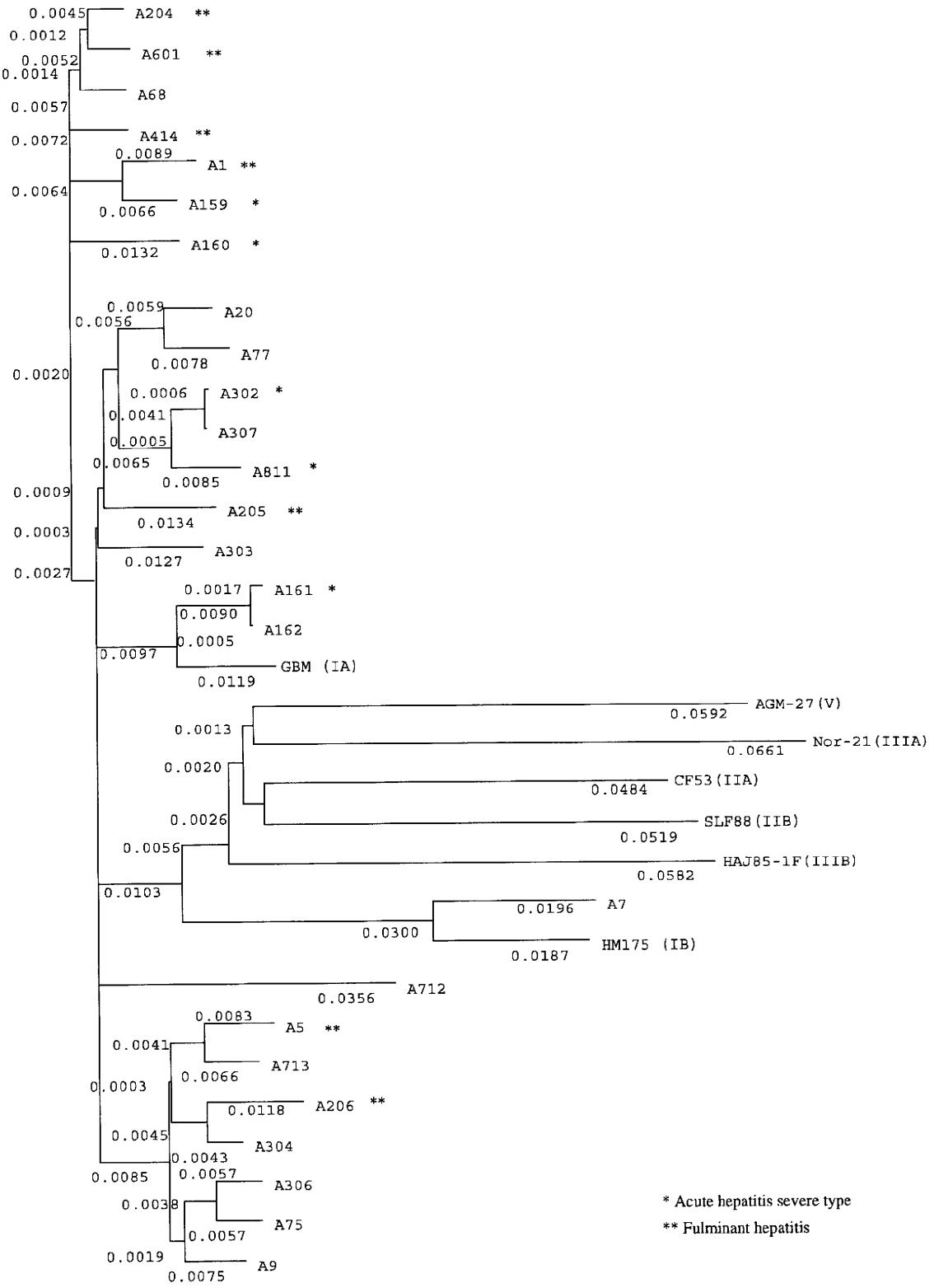

Fig. 2. Genetic relatedness between individual hepatitis A virus (HAV) of entire 2B and 2C recovered from 25 patients and HAV reference strains GBM (subgenotype IA), HM175 (subgenotype IB), CF53 (subgenotype IIA), SLF88 (subgenotype IIB), Nor-21 (subgenotype IIIA), HAJ85-1F (subgenotype IIIB) and AGM27 (genotype V). Numbers beside the phylogenetic roots are the results of bootstrap analyses.

Table 2. Clinical, biochemical and viral characteristics of six patients with fulminant and severe hepatitis located in the near parts of the phylogenetic tree

Patient	Diagnosis	Age/sex	Origin	Onset	Outcome	ALT (IU/L)	T-Bil (mg/dl)	PT (%)	IgM-HA (cut-off index)	Viral load (log copies/ml)	Days from onset
A204	FH	39/F	Tohoku	February 1990	Death	4470	5.3	10	3.8	ND	3
A601	FH	64/F	Shinetsu	January 1997	Death	12 500	7.0	13	2.9	3.7	9
A414	FH	49/M	Shinetsu	January 1989	Recovery	5276	26.3	13	+	5.0	7
A160	AHs	39/M	Kanto	June 1998	Recovery	9164	1.6	38	3.1	5.1	4
A1	FH	29/M	Kanto	March 1992	Recovery	1175	7.3	17	5.1	3.3	6
A159	AHs	50/M	Kanto	May 1998	Recovery	5655	2.5	20	4.6	4.6	5

Patient	Genotype	5′ NTR homology (%)	2B nt homology (%)	2C nt homology (%)
A204	IA	99.0	93.8	90.0
A601	IA	99.3	94.3	89.3
A414	IA	98.7	95.0	88.6
A160	IA	97.7	95.2	88.3
A1	IA	98.7	96.0	88.5
A159	IA	98.7	96.9	88.8

Homology, sequences were compared with wild-type HAV genotype IA strain GBM.
AH, acute hepatitis; AHs, acute hepatitis severe type; ALT, alanine aminotransferase; FH, fulminant hepatitis; 5′NTR, 5′-nontranslated region; ND, not done; nt, nucleotide; Ti-Bil, total bilirubin.

patients. Rezende *et al.* (29) reported that HAV-related liver failure is because of an excessive host response associated with a marked reduction in viral load, and there is a discrepancy between their data and ours. But they did not show the time points of serum sampling that represent critical data about viraemia in AH, and so we cannot discuss the discrepancy.

Thus, genetic variations not in one specific region but in 5′NTR, 2B and 2C might cooperatively influence replication of the virus and thereby affect virulence. Our findings are in accordance with the basic reports that the pathogenicity of HAV could be related to cooperative mutations within 5′NTR and P2 in cultured cells and simians, and the clinical finding that there has been only one report about a cluster of fulminant hepatitis A, unlike the many reports of clusters of fulminant hepatitis B.

Our current study suggests that both viral and host factors should be considered and examined when discussing the mechanisms responsible for the severity of hepatitis A. Further, we should examine several portions of the HAV genome including 5′NTR, 2B and 2C rather than focus on one specific region when analysing viral factors. Our study also suggests that vaccination should be considered all the more if HAV itself is involved in the pathogenicity of hepatitis A, because safe and extremely effective inactivated HAV vaccines are available.

References

1. Takahashi Y, Okuda K. Fulminant and subfulminant hepatitis in Japan. *Indian J Gastroenterol* 1993; **12**: 19–21.
2. Fujiwara K, Ehata T, Yokosuka O, *et al.* The recent increase of severe type A hepatitis in Chiba area. *Int Hepatol Commun* 1995; **3**: S37.
3. Fujiwara K, Yokosuka O, Ehata T, Imazeki F, Saisho H. PCR-SSCP analysis of 5′ nontranslated region of hepatitis A viral RNA: comparison with clinicopathological features of hepatitis A. *Dig Dis Sci* 2000; **45**: 2422–7.
4. Cohen JI, Ticehurst JR, Purcell RH, Buckler-White A, Baroudy BM. Complete nucleotide sequence of wild-type hepatitis A virus: comparison with different strains of hepatitis A virus and other picorna viruses. *J Virol* 1987; **61**: 50–9.
5. Cohen L, Bénichou D, Martin A. Analysis of deletion mutants indicates that the 2A polypeptide of hepatitis A virus participates in virion morphogenesis. *J Virol* 2002; **76**: 7495–505.
6. Teterina NL, Bienz K, Egger D, Gorbalenya AE, Ehrenfeld E. Induction of intracellular membrane rearrangements by HAV proteins 2C and 2BC. *Virology* 1997; **237**: 66–77.
7. Cohen JI, Rosenblum B, Ticehurst JR, *et al.* Complete nucleotide sequences of an attenuated hepatitis A virus: comparison with wild-type virus. *Proc Natl Acad Sci USA* 1987; **84**: 2497–501.
8. Graff J, Kasang C, Normann A, *et al.* Mutational events in consecutive passages of hepatitis A virus strain GBM during cell culture adaptation. *Virology* 1994; **204**: 60–8.
9. Zhang H, Chao S-F, Ping LH, *et al.* An infectious cDNA clone of a cytopathic hepatitis A virus: genomic regions associated with rapid replication and cytopathic effect. *Virology* 1995; **212**: 686–97.
10. Raychaudhuri G, Govindarajan S, Shapiro M, Purcell RH, Emerson SU. Utilization of chimeras between human (HM-175) and simian (AGM-27) strains of hepatitis A virus to study the molecular basis of virulence. *J Virol* 1998; **72**: 7467–75.
11. Durst RY, Goldsmidt N, Namestnick J, Safadi R, Ilan Y. Familial cluster of fulminant hepatitis A infection. *J Clin Gastroenterol* 2001; **32**: 453–4.

12. Fujiwara K, Yokosuka O, Ehata T, *et al.* Frequent detection of hepatitis A viral RNA in serum during the early convalescent phase of acute hepatitis A. *Hepatology* 1997; **26**: 1634–9.
13. Fujiwara K, Yokosuka O, Fukai K, *et al.* Analysis of full-length hepatitis A virus genome in sera from patients with fulminant and self-limited acute type A hepatitis. *J Hepatol* 2001; **35**: 112–9.
14. Fujiwara K, Yokosuka O, Ehata T, *et al.* Association between severity of type A hepatitis and nucleotide variations in the 5′ nontranslated region of hepatitis A virus RNA: strains from fulminant hepatitis have fewer nucleotide substitutions. *Gut* 2002; **51**: 82–8.
15. Fujiwara K, Yokosuka O, Imazeki F, *et al.* Analysis of the genotype-determining region of hepatitis A viral RNA in relation to disease severities. *Hepatol Res* 2003; **25**: 124–34.
16. Fujiwara K, Yokosuka O, Imazeki F, *et al.* Do high levels of viral replication contribute to fulminant hepatitis A? *Liver Int* 2005; **25**: 194–5.
17. Fujiwara K, Yokosuka O, Imazeki F, *et al.* Genetic analysis of hepatitis A virus protein 2C in sera from patients with fulminant and self-limited hepatitis A. *Hepatogastroenterology* 2007; **54**: 871–7.
18. Fujiwara K, Yokosuka O, Imazeki F, *et al.* Analysis of hepatitis A virus protein 2B in sera from various severities of hepatitis A. *J Gastroenterol* 2007; **42**: 560–6.
19. Okamoto H, Okada S, Sugiyama Y, *et al.* Detection of hepatitis C virus RNA by a two-step polymerase chain reaction with two pairs of primers deduced from the 5′-noncoding region. *Jpn J Exp Med* 1990; **60**: 215–22.
20. Kojima H, Yokosuka O, Fujiwara K, Imazeki F, Saisho H. Quantification of hepatitis A virus RNA in sera by real-time RT-PCR. *Proceeding of the 11th International Symposium on Viral Hepatitis and Liver Disease*, Sydney, 2004; 284–5.
21. Muraoka H. Clinical and epidemiological study on factors of serious development of viral hepatitis type A. *Nippon Shokakibyo Gakkai Zasshi* 1990; **87**: 1383–91.
22. Vento S, Garofano T, Renzini C, *et al.* Fulminant hepatitis associated with hepatitis A virus superinfection in patients with chronic hepatitis C. *N Engl J Med* 1998; **338**: 286–90.
23. Willner IR, Uhl MD, Howard SC, *et al.* Serious hepatitis A: an analysis of patients hospitalized during an urban epidemic in the United States. *Ann Intern Med* 1998; **128**: 111–4.
24. Day SP, Murphy P, Brown EA, *et al.* Mutations within the 5′ nontranslated region of hepatitis A virus RNA which enhance replication in BS-C cells. *J Virol* 1992; **66**: 6533–40.
25. Emerson SU, McRill C, Rosenblum B, Feinstone SM, Purcell RH. Mutations responsible for adaptation of hepatitis A virus to efficient growth in cell culture. *J Virol* 1991; **65**: 4882–6.
26. Emerson SU, Huang Y-K, McRill C, Lewis M, Purcell RH. Mutations in both the 2B and 2C genes of hepatitis A virus are involved in adaptation to growth in cell culture. *J Virol* 1992; **66**: 650–4.
27. Mirzayan C, Wimmer E. Genetic analysis of an NTP-binding motif in poliovirus polypeptide 2C. *Virology* 1992; **189**: 547–55.
28. Gosert R, Egger D, Bienz K. A cytopathic and a cell culture adapted hepatitis A virus strain differ in cell killing but not in intracellular membrane rearrangement. *Virology* 2000; **266**: 157–69.
29. Rezende G, Roque-Afonso AM, Samuel D, *et al.* Viral and clinical factors associated with the fulminant course of hepatitis A infection. *Hepatology* 2003; **38**: 613–8.

CLINICAL STUDIES

Ultrasound-guided treatments under low acoustic power contrast harmonic imaging for hepatocellular carcinomas undetected by B-mode ultrasonography

Hitoshi Maruyama, Masanori Takahashi, Hiroyuki Ishibashi, Hidehiro Okugawa, Shinichiro Okabe, Masaharu Yoshikawa and Osamu Yokosuka

Department of Medicine and Clinical Oncology, Chiba University Graduate School of Medicine, Chiba, Japan

Keywords
contrast agent – hepatocellular carcinoma – liver – Sonazoid™ – ultrasound

Correspondence
Hitoshi Maruyama, Department of Medicine and Clinical Oncology, Chiba University Graduate School of Medicine, 1-8-1, Inohana, Chuou-ku, Chiba 260-8670, Japan
Tel: +81 43 2262083
Fax: +81 43 2262088
e-mail: maru-cib@umin.ac.jp

Received 9 June 2008
Accepted 26 July 2008

DOI:10.1111/j.1478-3231.2008.01875.x

Abstract

Background/Aims: The aim was to examine the efficacy of contrast-enhanced ultrasound (US) with Sonazoid™ to demonstrate ultrasonically unrecognizable hypervascular hepatocellular carcinoma (HCC) and apply percutaneous US-guided treatments. *Methods:* The subjects of this prospective study were 44 cirrhotic patients with 55 hypervascular lesions (12.7 ± 4.5 mm) found by contrast-enhanced computed tomography but unrecognized by non-contrast US. Contrast-enhanced US was performed to demonstrate these hepatic lesions after an intravenous injection of Sonazoid™ (0.0075 ml/kg). The sonograms in both the early phase (for 1 min after injection) and the late phase (5–10 min after) were taken in the harmonic imaging mode under a low mechanical index (0.24–0.3). *Results:* Fifty-three lesions were demonstrated by contrast-enhanced US, 52 with positive enhancement in the early phase and 44 with negative enhancement in the late phase. Percutaneous US-guided treatments were successfully performed for 42 lesions (ethanol injection in 20 and radiofrequency ablation in 22) in 32 patients with reference to contrast-enhanced US findings. Six patients were treated by transarterial chemoembolization alone because they had more than three lesions in the liver. In the remaining seven lesions in six patients, six were diagnosed as non-HCC lesions: five with vascular abnormalities such as arterioportal or arteriovenous communication and the other one with benign lesion in alcoholic liver disease. These six lesions and one HCC lesion with severe liver damage were followed up without any treatment. *Conclusions:* As the detectability of ultrasonically unrecognizable hypervascular HCC improved by contrast-enhanced US with Sonazoid™, a wider application of percutaneous US-guided treatments may be possible.

Hepatocellular carcinoma (HCC) is increasing worldwide and is one of the most common carcinomas in the eastern part of Asia (1). As the prognosis of cirrhotic patients depends on the occurrence and progression of HCC, management of this neoplasm is a major issue in clinical practice. However, surgical treatment is not always an appropriate choice, as the majority of HCC patients have poor liver function and recurrence is not rare (2–4).

Real-time observation is the most significant point to be emphasized in the clinical use of ultrasound (US), and the percutaneous US-guided technique is a reasonable procedure for the treatment of HCC with minimal invasiveness (5–9). Although these methods require demonstration of focal hepatic lesions by US, this is not always easy because of deformity and/or coarse parenchymal echo in cirrhotic liver, and modified echo patterns as a result of previous treatments (10, 11). Contrast-enhanced US with Levovist facilitated the application of percutaneous US-guided treatments by successful localization in about 75% of ultrasonically invisible hypervascular HCCs (12). However, the utility of second-generation microbubble contrast agents for the localization of such focal hepatic lesions has not been established.

Second-generation microbubble contrast agents have acquired stability of microbubble by homogenization of particle size distribution in comparison with earlier agents (13, 14). The combination of second-generation contrast agents with harmonic imaging mode under lower mechanical index (MI) may provide US images with an improved signal-to-noise ratio, and a higher detection rate of focal lesions in the liver is expected (15, 16).

Sonazoid™ is a newly developed perflubutane US contrast agent (17–19). The microbubble has the characteristic property of accumulation in the Kupffer cell, and it is the largest difference between this agent and SonoVue, a popular agent in Europe. Application of Sonazoid-enhanced sonograms produced by accumulated microbubble as well as circulating microbubble may contribute greatly to the detection of focal hepatic lesions. With this background, the present study was designed to examine the efficacy of contrast-enhanced US with the new perflubutane microbubble agent Sonazoid™ in the visualization of ultrasonically unrecognized hepatic lesions that had a hypervascular appearance on contrast-enhanced computed tomography (CT), for the application of percutaneous US-guided treatments in cirrhotic patients.

Material and methods

Patients

Between February 2007 and May 2008, a prospective study was performed to examine the efficacy of contrast-enhanced US with Sonazoid™ (GE Healthcare, Oslo, Norway) to

demonstrate hypervascular hepatic lesions seen on contrast-enhanced CT but not by non-contrast US in our department. The following criteria were used for study enrolment: (i) cirrhotic patients with solitary or multiple focal hypervascular lesions found by contrast-enhanced CT taken for the surveillance of HCC, (ii) radiological diagnosis of hepatic lesions was HCC on CT images, (iii) non-contrast US could not recognize the hepatic lesions and (iv) patients without egg allergy, a contraindication of Sonazoid™. In this study period, there were 1286 patients who received a contrast-enhanced CT examination for the surveillance of HCC in our department. Among them, the subjects of this study were 44 cirrhotic patients with 55 hypervascular lesions, and they consisted of 28 males and 16 females, aged 68.2 ± 9.2 years (range 33–78). The diagnosis of liver cirrhosis was based on imaging findings with clinical symptoms and biochemistry findings in all patients, with six patients positive for hepatitis B virus surface antigen, 33 positive for hepatitis C virus antibody, two with alcohol abuse and three patients cryptogenic. The total number of hypervascular lesions in all patients was 55 (one in 37 patients, two in four patients, three in two patients and four in one patients) with a size ranging from 5 to 24 mm (12.7 ± 4.5 mm) on CT images. The serum α-fetoprotein level ranged from 1.9 to 991.1 ng/ml, being normal in 20 patients and abnormal in 24 patients (109.6 ± 209.8). Nine patients had no previous HCC diagnosis or treatment, and the other 35 patients had treatment histories for HCC: percutaneous ethanol injection (PEI) in five, radiofrequency ablation (RFA) in 17, transarterial chemoembolization (TACE) in five and TACE followed by PEI in eight. Hypervascular lesions were located at treated sites in 43 lesions in 34 patients and at untreated sites in 12 lesions in 10 patients. As non-contrast-enhanced greyscale US examination had failed to detect any of the lesions, a percutaneous needle biopsy was not performed at that time. This study was approved by the ethics committee of our institute, and informed written consent was obtained from all patients.

Ultrasound examination

US examination was performed using SSA-770A and 790A (APLIO; Toshiba, Tokyo, Japan) with a 3.75 MHz convex or microconvex probe. After non-contrast greyscale US (tissue harmonic imaging, 2.5/5.0, 14–27 Hz) and colour Doppler imaging, contrast-enhanced US was carried out in the pulse subtraction harmonic imaging mode with an MI level from 0.24 to 0.3 to observe the suspected tumour location area as estimated from the contrast-enhanced CT images. Gain was adjusted at an optimal level, and the dynamic range was set at 65 dB for non-contrast US and 45-55 dB for contrast-enhanced US. Observation of non-contrast images and the late-phase (5–10 min after the injection of Sonazoid™) images was performed by both an intercostal scan and a subcostal scan for the right lobe, and both a sagittal scan and a transverse scan for the left lobe, under possible breath holding. Each scan was completed with gentle and reciprocatory movement of the probe, right side to left side and left side to right side, or caudal side to cranial side and cranial side to caudal side. As for the early phase (from onset of contrast enhancement to 1 min), a scan plane that allowed the most stable demonstration was carefully selected and contrast-enhanced findings were observed by tilting the probe under possible breath holding.

The contrast agent Sonazoid™ (perflubutane microbubbles with a median diameter of 2–3 μm) was used at a dose of 0.0075 ml/kg by a manual bolus injection following a flush with 3.0 ml of normal saline solution, once for the observation of each lesion (once in 37 patients, twice in four patients, three times in two patients and four times in one patient). The subsequent injection was given after the disappearance of the previous enhancement. The operators for US examinations were H. M. (18-year experience) in 20 patients, M. T. (6-year experience) in 14 patients, H. I. (6-year experience) in six patients and H. O. (8-year experience) in four patients. All US images recorded digitally were reviewed at a later date by H. O., and contrast-enhanced findings in the hepatic lesions were noted in comparison with those in surrounding liver parenchyma as positive, equal or negative enhancement. Hepatic lesions with either positive enhancement in the early-phase image or negative enhancement in the late-phase image were considered to be localized target lesions. Furthermore, the presence or absence of contrast enhancement in the intrahepatic portal vein was also noted at the late phase, based on the microbubble-disappearance time (20).

Contrast-enhanced computed tomography and computed tomography angiography

Contrast-enhanced CT with a dynamic study was performed in all patients using Lightspeed ultra16 (GE Yokogawa Medical Systems, Hino, Japan) with an injection of 100 ml of a contrast medium (Iopamiron 350; Nihon Schering, Osaka, Japan) at 3 ml/s from the antecubital vein by a mechanical power injector. Imaging was performed with a 30-s delay between contrast medium administration and start of imaging for the hepatic artery-dominant phase, an 80-s delay for the portal vein-dominant phase and a 180-s delay for the equilibrium phase. Contrast-enhanced CT was performed again in patients who received treatment for hepatic lesions to evaluate the therapeutic response. Findings of contrast-enhanced CT both before and after the treatment were evaluated blindly by S. O. to confirm the therapeutic effect and whether the lesion contrast-enhanced US demonstrated was the lesion detected on contrast-enhanced CT.

CT angiography was performed using Infinix Active Aquilion Type (Toshiba) with an injection of 15 ml of contrast medium (Iopamiron 300; Nihon Schering) at 3 ml/s via a catheter placed at the common hepatic artery by a mechanical power injector. Imaging was performed with a 2-s and an 8-s delay between contrast medium administration and start of imaging for the artery-dominant phase. This imaging was planned after a contrast-enhanced US examination and applied in 27 patients according to the standard protocol in our department: in patients with the initial treatment for HCC, patients with solitary or multiple lesions requiring TACE because of the lesions considered to be technically difficult for percutaneous needle advancement and patients with hepatic lesions not demonstrated by contrast-enhanced US. Findings of CT angiography were evaluated blindly by M. Y.

Ultrasound-guided puncture for hepatic lesions

Biopsy for hepatic lesions was performed by a 21-gauge needle (Sonopsy; Hakko, Tokyo, Japan), PEI was performed with a 22-gauge Chiba needle (Top, Tokyo, Japan) and RFA was performed with a 17-gauge cool-tip radio frequency electrode (Radionics, Burlington, MA, USA). All US-guided procedures were performed using a convex or microconvex probe with a specially designed attachment. Percutaneous needle biopsy was applied in patients with the initial diagnosis or treatment for

HCC, according to the standard protocol in our department. When hepatic lesions became recognized on the non-contrast sonogram in reference to the contrast-enhanced US findings, US-guided punctures were conducted under non-contrast US. However, when hepatic lesions were not clearly recognized on the non-contrast sonogram regardless of the reference of contrast-enhanced US findings, these US-guided procedures were conducted under contrast-enhanced US with an additional injection of Sonazoid™.

Statistical analysis

All data were expressed as mean ± standard deviation or percentage. Statistical significance was determined using Fisher's exact test, and significance was considered at $P < 0.05$. Statistical analysis was performed using the SPSS package (version 13.0J; SPSS Inc., Chicago, IL, USA).

Results

Detection of focal hepatic lesions by contrast-enhanced ultrasound

Fifty-two lesions showed a positive enhancement in the early phase and 44 lesions showed a negative enhancement in the late phase (Table 1), with phasic detectability being significantly higher in the early phase (52/55) than that in the late phase (44/55, $P = 0.0221$). Consequently, 53 lesions were demonstrated by contrast-enhanced US with Sonazoid™, yielding a detection rate of 96.4% (Figs 1 and 2). Twenty-one of the 55 lesions (38.2%) were < 10 mm, with the detection rate between lesions < 10 mm and ≥ 10 mm not being significantly different (Fig. 3). In addition, 13 of the 55 lesions (23.6%) lesions were located deeper than 8 cm from the skin surface (Fig. 3). Contrast enhancement in the intrahepatic portal vein at the late phase was still visible in 33 (60%) patients with 37 lesions and in 11 (29.7%) of the 37 lesions showing an equal enhancement to the surrounding liver parenchyma in this phase. Percutaneous needle biopsy was performed for 10 of the successfully demonstrated 53 lesions under the non-contrast sonogram. Their diagnosis was seven moderately differentiated HCC (7, 10, 13, 15, 18, 20 and 24 mm), two well-differentiated HCC (10, 12 mm) and one benign nodule (13 mm) found in alcoholic liver disease.

Clinical course after contrast-enhanced ultrasound

Percutaneous US-guided treatments were successfully performed in 42 lesions (PEI in 20 and RFA in 22) in 32 patients, and all hypervascular hepatic lesions changed to hypovascular appearances on contrast-enhanced CT images after the treatment. Thus, treatment effectiveness was confirmed on contrast-enhanced CT images and this was the evidence that the lesion contrast-enhanced US demonstrated was the lesion detected on contrast-enhanced CT. Six patients, each patient having one hypervascular lesion on contrast-enhanced CT, were treated by TACE alone because CT angiography showed more than three lesions in the liver. In the remaining seven lesions in six patients, six were diagnosed as non-HCC lesions. Two lesions were diagnosed as arterioportal communication by both CT angiography and contrast-enhanced US. Two lesions undetected by contrast-enhanced US were diagnosed as a vascular abnormality such as arterioportal communication because HCC was ruled out by CT angiography and the findings on subsequent contrast-enhanced CT showed no change in their clinical course, one case after 11 months and the other after 1 year (Fig. 2). One lesion was diagnosed as arteriovenous communication by contrast-enhanced US, and the other case with a benign lesion in alcoholic liver disease by a percutaneous needle biopsy. These six lesions and one lesion with severe liver damage were followed up without any treatment, and the findings of the former six lesions on contrast-enhanced CT did not change during the clinical course of 8.4 ± 1.9 (5–14) months.

Table 1. Contrast-enhanced ultrasound findings of hepatic lesions in each phase

Enhanced findings	Early phase	Late phase
Positive	52	0
Equal	3	11
Negative	0	44

Fifty-two lesions showed positive enhancement in the early phase and 44 lesions showed negative enhancement in the late phase, with phasic detectability being significantly higher in the early phase (52/55) than in the late phase (44/55, $P = 0.0221$). Consequently, 53 lesions were demonstrated by contrast-enhanced ultrasound with Sonazoid™, a detection rate of 96.4%.

Discussion

Percutaneous US-guided treatments that require obvious demonstration of focal hepatic lesions on sonograms are minimally invasive and effective for HCC. However, a potential pitfall sometimes hinders the wider application of the technique, because visualization of focal hepatic lesions is not easy in cirrhotic patients (10, 11). To overcome this problem for the application of percutaneous US-guided treatments, some ingenious development is awaited.

As shown in the present study, the majority of ultrasonically unrecognized small hepatic lesions with a hypervascular appearance on contrast-enhanced CT were successfully demonstrated by contrast-enhanced US with Sonazoid™. Furthermore, the results suggested that our technique might be less dependent on the size or the location of the hepatic lesions.

Although all the hepatic lesions had a hypervascular appearance on contrast-enhanced CT, three of the 55 lesions showed equal enhancement on the early-phase sonograms. This might be explained by the saturation by contrast enhancement of the surrounding parenchyma owing to the inappropriate scan timing for the hepatic lesion, because the onset of contrast enhancement after the injection of the microbubble agent varies case by case and breath holding is sometimes inadequate. Furthermore, we had to observe early-phase images while searching for the lesions with positive enhancement by tilting the probe. Therefore, an inevitable delayed observation might account for the equal enhancement on the early-phase sonograms in these three hepatic lesions.

Meanwhile, the late-phase observation was relatively easy to perform, as with repeated observation it was possible to depict the negatively enhanced lesions in the liver parenchyma with homogeneous enhancement. However, detectability of hepatic lesions in the late phase was significantly lower than that in the early phase, and 11 of the 55 lesions had equal enhancement in the late phase. It is reported that Sonazoid™ microbubbles are captured by Kupffer cells in the liver (18), while retained intrahepatic microbubble circulation was found in approximately half of the subjects in the late phase in the present study.

Liver International (2009)

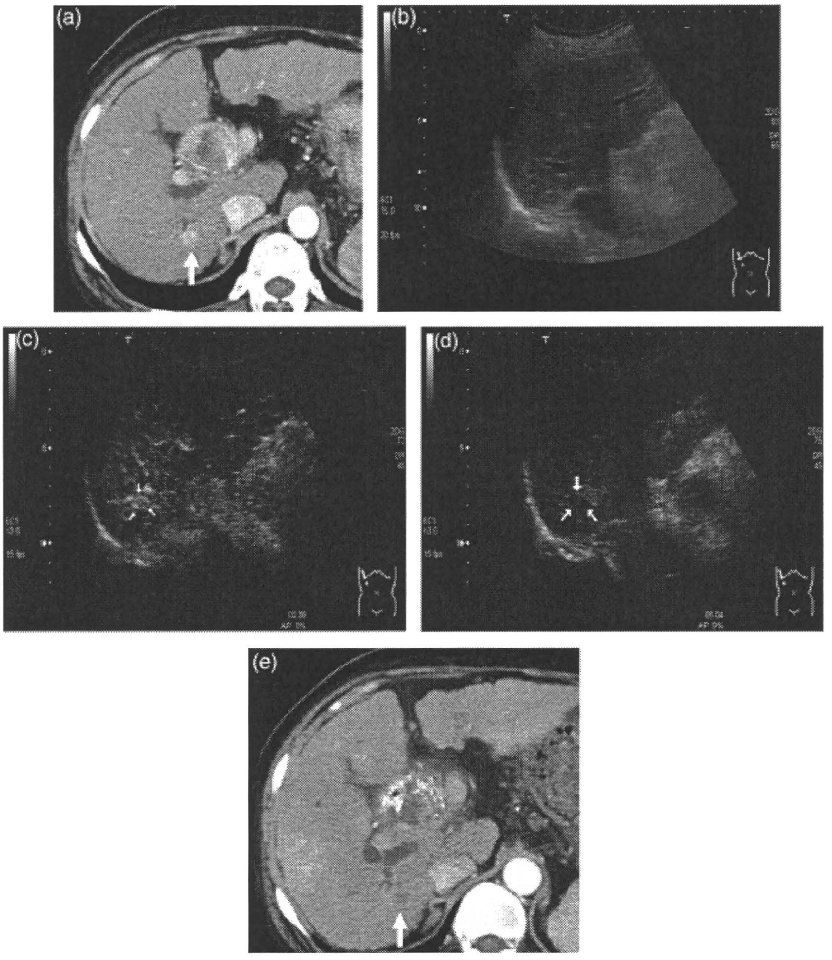

Fig. 1. Fifty-seven-year-old female, hepatitis B virus-related liver cirrhosis. (a) Contrast-enhanced computed tomography (CT) image. A hypervascular lesion (arrow) considered to be hepatocellular carcinoma was demonstrated on CT image. (b) Non-contrast sonogram. Hepatic lesion corresponding to CT findings was not recognized on the sonogram before enhancement. (c) Contrast-enhanced sonogram in the early phase. A hypervascular lesion was demonstrated on the sonogram after enhancement (arrows). (d) Contrast-enhanced sonogram in the late phase. The lesion showed negative enhancement in this phase (arrows). (e) Contrast-enhanced CT image after a percutaneous ethanol injection. Hepatic lesion showed a hypovascular appearance after the treatment (arrow).

Therefore, the phase from 5 to 10 min after the injection of Sonazoid™ might not be produced by accumulated microbubbles alone, and the equal enhancement findings in some hepatic lesions in the late phase might be explained by the residual intravascular enhancement. In any event, observation both in the early phase and in the late phase would be necessary for detection of these hepatic lesions.

The previous study showed that Levovist (Schering AG, Berlin, Germany), a first-generation US contrast agent, improved the localization of ultrasonically unrecognized hypervascular lesions in the liver (12). However, the detection rate of 75% was lower than that with Sonazoid™. An appropriate imaging mode for Levovist was based on Doppler mode, which suffers from artefacts, and it requires the setting of regions of interest whose size vary inversely to the frame rate. In addition, contrast-enhanced US images were observed by a low frame rate of 4–8 Hz in the early phase and intermittent scanning with 1 frame/s in the late phase, imaging sequences suitable for Levovist. Thus, improved signal-to-noise ratio and real-time performance may be the advantages of our technique with Sonazoid™, which resulted in increased detectability of hepatic lesions in comparison with the results using Levovist. Another study showed that RFA was sufficiently achieved using Sonazoid™ for undetected lesions by conventional US (19). However, that study had some differences from ours, because it included large-sized tumours and the use of a combined method with low acoustic power and high acoustic power according to the phase. Although an optimal acoustical condition for Sonazoid™ has still not been established, our technique under a low-MI condition throughout the examination may be more simple and convenient. Obviously, the establishment of appropriate imaging sequences would be helpful for the standardization and popularization of contrast-enhanced US with Sonazoid™.

We failed to demonstrate two focal hepatic lesions in our study, which were fortunately considered to be arterioportal communications. In fact, there were five patients with vascular abnormalities, so-called 'pseudo-lesions', that sometimes confuse the differentiation from hypervascular HCC on contrast-enhanced CT (21–23). The reasons for detection failure of these

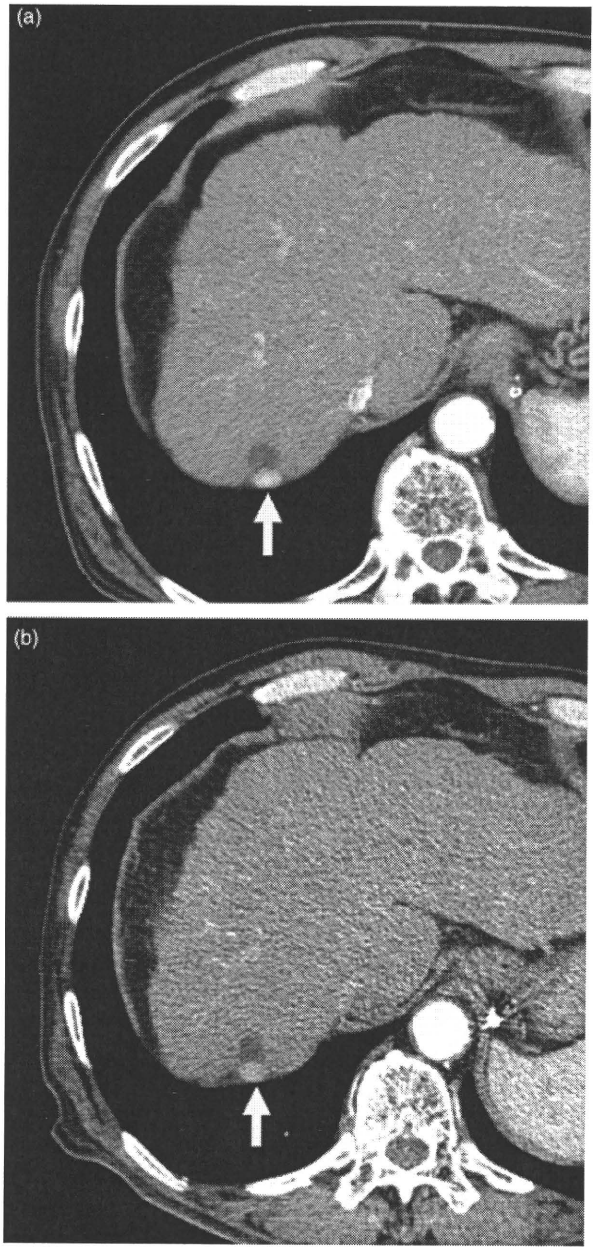

Fig. 2. Sixty-eight-year-old male, liver cirrhosis caused by alcohol abuse. (a) Contrast-enhanced computed tomography (CT) image on 10 March 2007. Contrast-enhanced CT image showed a hypervascular lesion (arrow) considered to be recurrence of hepatocellular carcinoma around the treated area. This lesion was not demonstrated by either non-contrast ultrasound (US) or contrast-enhanced US. (b) Contrast-enhanced CT image on 22 February 2008. Hypervascular lesion (arrow) did not show remarkable changes in form and size in comparison with that in the previous CT image. This hypervascular lesion was considered to be a vascular abnormality such as arterioportal communication.

lesions may be the difficulty of sonographical demonstration because of the location and/or the pathological property of the vascular abnormality. Although our technique achieved quite a high detection rate for malignant hepatic lesions, improvement

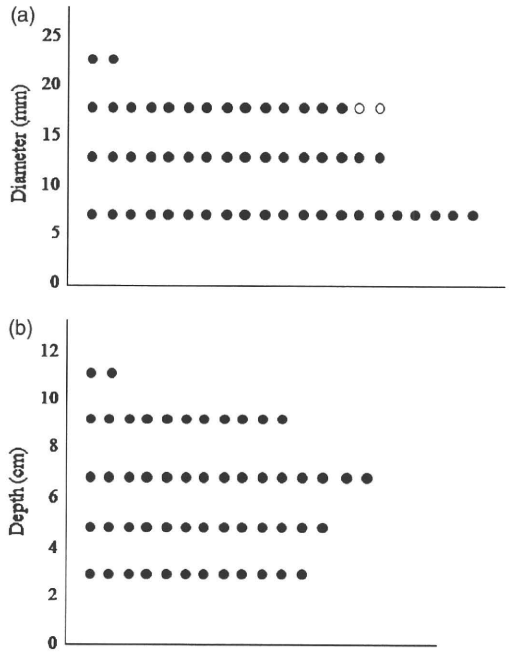

Fig. 3. (a) Distribution of hepatic lesions in relation to the diameter of the tumour. Twenty-one of the 55 lesions (38.2%) were < 10 mm. Closed circles: detected lesions [diameter measured by ultrasound (US)]. Open circles: undetected lesions (diameter measured by computed tomography). (b) Distribution of hepatic lesions in relation to the depth of the tumour location. Thirteen of the 55 lesions (23.6%) were located deeper than 8 cm from the skin surface. Two lesions undetected by contrast-enhanced US were not included because their depth was not measured on sonograms.

in diagnostic ability for such vascular abnormalities would be a worthwhile mission for contrast-enhanced US development in the near future.

There was one benign hepatic lesion histologically proven in one patient with alcoholic liver disease. It is known that hypervascular hepatic lesions do not always reflect the fact that the final diagnosis of the nodule is HCC in heavy drinkers (24). The ring-shaped appearance on liver-specific contrast-enhanced sonograms with Levovist is reported to be a useful sign for the diagnosis of a benign nodule in heavy drinkers (25). However, the benign lesion in the present study did not show this sign in the late phase. Although this might be explained by the very small size of the lesion in which the ring-shaped appearance was hard to recognize and/or the difference of microbubble property between Levovist and Sonazoid™, further studies would be needed to investigate this issue.

CT-guided needle puncture is also an effective method for hepatic tumours not recognized by US examination (26–29). However, it is not an easy procedure, and it requires radiation exposure and is time consuming. As contrast-enhanced US with Sonazoid™ could provide quite sufficient detectability of ultrasonically unrecognizable hepatic lesions, the application of CT-guided treatment may be confined to cases not demonstrated by contrast-enhanced US.

Cost, time and manpower are not negligible aspects to discuss the value of physical examination. As for the cost of contrast agent, one vial of Sonazoid™ (about US$100) is usually enough for one patient, because 2.0 ml of Sonazoid™

Liver International (2009)

solution is available by one vial and each injection was applied at a dose of 0.0075ml/kg in our method. Next, contrast-enhanced US examination is not a costless work, because it needs an assistant for the preparation and injection of a contrast agent, in addition to the US operator. Furthermore, as about 10-min observation was required for both the early and the late phase in our study, contrast-enhanced US may not be as brief as conventional US. However, the benefit and safety of contrast-enhanced US with Sonazoid™ would outweigh the cost manpower and time required in this procedure.

The present study has the limitation that the diagnosis of all hepatic lesions was not proven histologically. The European Association for the Study of the Liver has documented that nodules larger than 2 cm with an arterial hypervascular pattern by two imaging techniques are diagnosed as HCC without pathological findings, and sampling error could not be denied in the needle biopsy for small hepatic lesions (3, 30). Therefore, histological proof for all hepatic lesions may not be indispensable in our study. However, various kinds of hypervascular hepatic tumours such as haemangioma or focal nodular hyperplasia might have been included, although their diagnosis on contrast-enhanced CT was HCC. A second limitation was that there were no additional lesions detected by contrast-enhanced US, because the observation of contrast enhancement was limited to the tumour area estimated by contrast-enhanced CT. In fact, we had six patients treated by TACE alone because CT angiography following contrast-enhanced US showed more than one lesion that was presented on contrast-enhanced CT in the liver. Although the early-phase observation for multiple hepatic lesions may be difficult, scanning for other areas of the liver in the late phase might be helpful for detecting additional lesions as hypo-enhancement lesions. As these six patients were, after all, treated not by US-guided treatment but by TACE, demonstration of additional lesions might not affect the therapeutic strategy for them. However, this point may be improved with an increase in the detectability of hepatic lesions by contrast-enhanced US.

In conclusion, the detection rate of ultrasonically unrecognized hypervascular HCC was improved by contrast-enhanced US with Sonazoid™. This technique may allow the wider application of percutaneous US-guided treatments, which are minimally invasive procedures, in patients with HCC.

References

1. Bosch FX, Ribes J, Borras J. Epidemiology of primary liver cancer. *Semin Liver Dis* 1999; **19**: 271–85.
2. Okuda K. Hepatocellular carcinoma. *J Hepatol* 2000; **32**: 225–37.
3. Bruix J, Sherman M, Llovet JM, *et al.* Clinical management of hepatocellular carcinoma. Conclusions of the Barcelona-2000 EASL conference. European Association for the Study of the Liver. *J Hepatol* 2001; **35**: 421–30.
4. Ryu M, Shimamura Y, Kinoshita T, *et al.* Therapeutic results of resection, transcatheter arterial embolization and percutaneous ethanol injection in 3225 patients with hepatocellular carcinoma: a retrospective multicenter study. *Jpn J Clin Oncol* 1997; **27**: 251–7.
5. Livraghi T, Bolondi L, Lazzaroni S, *et al.* Percutaneous ethanol injection in the treatment of hepatocellular carcinoma in cirrhosis. A study on 207 patients. *Cancer* 1992; **69**: 925–9.
6. Goldberg SN, Gazelle GS, Solbiati L, Rittman WJ, Mueller PR. Radiofrequency tissue ablation: increased lesion diameter with a perfusion electrode. *Acad Radiol* 1996; **3**: 636–44.
7. Giorgio A, Tarantino L, de Stefano G, *et al.* Percutaneous sonographically guided saline-enhanced radiofrequency ablation of hepatocellular carcinoma. *Am J Roentgenol* 2003; **181**: 479–84.
8. Lencioni RA, Allgaier HP, Cioni D, *et al.* Small hepatocellular carcinoma in cirrhosis: randomized comparison of radio-frequency thermal ablation versus percutaneous ethanol injection. *Radiology* 2003; **228**: 235–40.
9. Ebara M, Okabe S, Kita K, *et al.* Percutaneous ethanol injection for small hepatocellular carcinoma: therapeutic efficacy based on 20-year observation. *J Hepatol* 2005; **43**: 458–64.
10. Takayasu K, Muramatsu Y, Asai S, *et al.* CT fluoroscopy-assisted needle puncture and ethanol injection for hepatocellular carcinoma: a preliminary study. *Am J Roentgenol* 1999; **173**: 1219–24.
11. Sato M, Watanabe Y, Tokui K, *et al.* CT-guided treatment of ultrasonically invisible hepatocellular carcinoma. *Am J Gastroenterol* 2000; **95**: 2102–6.
12. Maruyama H, Kobayashi S, Yoshizumi H, *et al.* Application of percutaneous ultrasound-guided treatment for ultrasonically invisible hypervascular hepatocellular carcinoma using microbubble contrast agent. *Clin Radiol* 2007; **62**: 668–75.
13. Goldberg BB. *Ultrasound Contrast Agents*. London: Martin Dunitz Ltd, 1997; 169.
14. Morel DR, Schwieger I, Hohn L, *et al.* Human pharmacokinetics and safety evaluation of SonoVue, a new contrast agent for ultrasound imaging. *Invest Radiol* 2000; **35**: 80–5.
15. Maruyama H, Matsutani S, Saisho H, Mine Y, Yuki H, Miyata K. Extra-low acoustic power harmonic images of the liver with Perflutren: novel imaging for real-time observation of liver perfusion. *J Ultrasound Med* 2003; **22**: 931–8.
16. von Herbay A, Vogt C, Willers R, Haussinger D. Real-time imaging with the sonographic contrast agent SonoVue: differentiation between benign and malignant hepatic lesions. *J Ultrasound Med* 2004; **23**: 1557–68.
17. Marelli C. Preliminary experience with NC100100, a new ultrasound contrast agent for intravenous injection. *Eur Radiol* 1999; **9**(Suppl. 3): S343–6.
18. Watanabe R, Matsumura M, Munemasa T, Fujimaki M, Suematsu M. Mechanism of hepatic parenchyma-specific contrast of microbubble-based contrast agent for ultrasonography: microscopic studies in rat liver. *Invest Radiol* 2007; **42**: 643–51.
19. Numata K, Morimoto M, Ogura T, *et al.* Ablation therapy guided by contrast-enhanced sonography with sonazoid for hepatocellular carcinoma lesions not detected by conventional sonography. *J Ultrasound Med* 2008; **27**: 395–406.
20. Maruyama H, Matsutani S, Okugawa H, *et al.* Microbubble disappearance-time is the appropriate timing for liver-specific imaging after injection of Levovist. *Ultrasound Med Biol* 2006; **32**: 1809–15.
21. Yu JS, Kim KW, Sung KB, *et al.* Small arterial-portal venous shunts: cause of pseudolesions at hepatic imaging. *Radiology* 1997; **203**: 737–42.
22. Kim TK, Choi BI, Han JK, *et al.* Nontumorous arterioportal shunt mimicking hypervascular tumor in cirrhotic liver: two-phase spiral CT findings. *Radiology* 1998; **208**: 597–603.
23. Brancatelli G, Baron RL, Peterson MS, *et al.* Helical CT screening for hepatocellular carcinoma in patients with cirrhosis: frequency and causes of false-positive interpretation. *Am J Roentgenol* 2003; **180**: 1007–14.
24. Kim SR, Maekawa Y, Ninomiya T, *et al.* Multiple hypervascular liver nodules in a heavy drinker of alcohol. *J Gastroenterol Hepatol* 2005; **20**: 795–9.
25. Maruyama H, Matsutani S, Kondo F, *et al.* Ring-shaped appearance on liver-specific image with Levovist: a characteristic enhancement

pattern for hypervascular benign nodule in the liver of heavy drinkers. *Liver Int* 2006; **26**: 688–94.
26. Schweiger GD, Brown BP, Pelsang RE, *et al.* CT fluoroscopy: technique and utility in guiding biopsies of transiently enhancing hepatic masses. *Abdom Imaging* 2000; **25**: 81–5.
27. Shibata T, Iimuro Y, Yamamoto Y, *et al.* CT-guided transthoracic percutaneous ethanol injection for hepatocellular carcinoma not detected with US. *Radiology* 2002; **223**: 115–20.
28. Kirchner J, Kickuth R, Laufer U, *et al.* CT fluoroscopy-assisted puncture of thoracic and abdominal masses: a randomized trial. *Clin Radiol* 2002; **57**: 188–92.
29. Adam A, Hatzidakis A, Hamady M, *et al.* Percutaneous coil placement prior to radiofrequency ablation of poorly visible hepatic tumors. *Eur Radiol* 2004; **14**: 1688–91.
30. Nakashima T, Kojiro M. *Hepatocellular Carcinoma*. Tokyo: Springer-Verlag, 1987.

Scandinavian Journal of Gastroenterology, 2009; 44: 872–877

informa
healthcare

ORIGINAL ARTICLE

Quantification of hepatitis C amino acid substitutions 70 and 91 in the core coding region by real-time amplification refractory mutation system reverse transcription-polymerase chain reaction

SHINGO NAKAMOTO, TATSUO KANDA, YUTAKA YONEMITSU, MAKOTO ARAI, KEIICHI FUJIWARA, KENICHI FUKAI, FUMIHIKO KANAI, FUMIO IMAZEKI & OSAMU YOKOSUKA

Department of Medicine and Clinical Oncology, Graduate School of Medicine, Chiba University, Chiba, Japan

Abstract

Objective. The effects of hepatitis C virus (HCV) sequence variations on the success of antiviral therapy or the development of hepatocellular carcinoma (HCC) are complex for many reasons. Recently, there have been several reports on the effects of genotype 1b HCV core amino acid substitutions 70 and/or 91 on the outcome of antiviral therapies and the clinical course. The purpose of this study was to establish real-time amplification refractory mutation system (ARMS) reverse transcription (RT)-polymerase chain reaction (PCR) assays for easy detection of these HCV mutations. ***Material and methods.*** Plasmids p-core-W, including the wild-type HCV core coding region (70R and 91L), and p-core-M, including the mutant-type HCV core (70Q and 91M), were constructed by cloning and PCR-based mutagenesis for control vector of the wild-type core and that of the mutant core, respectively. Using serially diluted forms of these vectors, SyBr Green-based real-time ARMS RT-PCR detection with each of the specific primer pairs was performed. ***Results.*** Each primer could clearly distinguish the difference between p-core-W and p-core-M at the same copy numbers. Concerning substitution 70, the ratios 100:1, 10:1, 1:1, 1:10, and 1:100 of p-core-W versus p-core-M could be distinguished, while for substitution 91, the ratios 100:1, 10:1, 1:1, 1:10, 1:100, and 1:1000 could be distinguished, confirming the sensitivity and specificity of the assay. ***Conclusions.*** This method could be a useful alternative for the detection of genotype 1b HCV core amino acid substitutions 70 and 91 and be reliably applied for rapid screening.

Key Words: *ARMS, core, HCV, interferon response, real-time PCR*

Introduction

More than 170 million people world-wide are chronically infected with hepatitis C virus (HCV), which can lead to hepatic cirrhosis and hepatocellular carcinoma (HCC) [1]. Treatment with peginterferon and ribavirin for 24–48 weeks can result in a sustained loss of serum HCV-RNA (termed a sustained virological response (SVR)), with resolution of chronic hepatitis in approximately half of the patients [2]. Several new, potent HCV protease and polymerase inhibitors have been described recently, but none of them are available for therapeutic use.

The genomic region encoding the HCV core protein is located between amino acids 1 and 191 and is likely to be the first gene product synthesized due to its localization at the 5′ end of the HCV polyprotein transcript [3]. The core protein has an ability to interact with the viral genomic region to form nucleocapsids [4], and the presence of a putative DNA-binding motif, nuclear localization signals, phosphorylation sites, and a nucleocytoplasmic localization of the core protein suggest its possible function as a gene regulatory protein [3,5]. In many previous studies it has been suggested that the HCV core protein may be important in hepatocarcinogenesis and interferon signaling [3,6–8].

HCV genotype 1b is a major genotype (~70%) in Japan. HCV genotype 1 is one of the most refractory to interferon treatment with or without ribavirin. It has been reported that its response to interferon

Correspondence: Tatsuo Kanda, MD, PhD, Department of Medicine and Clinical Oncology, Graduate School of Medicine, Chiba University, 1-8-1 Inohana, Chuo-ku, Chiba 260-8677, Japan. Tel: +81 43 2262 086. Fax: +81 43 2262 088. E-mail: kandat-cib@umin.ac.jp

(Received 5 February 2009; accepted 29 March 2009)

ISSN 0036-5521 print/ISSN 1502-7708 online
DOI: 10.1080/00365520902937362

monotherapy is affected by HCV NS5A gene diversity [9]. Thus, sequence diversity may predict the response to the combination therapy of peginterferon and ribavirin. Furthermore, ribavirin has different antiviral effects from those of interferon [10]. An approach to the prediction of treatment against hepatitis C in patients who do not have SVR is urgently needed. Several reports suggest that HCV amino acid substitutions 70 and 91 in the core coding region affect the results of combination therapies of interferon and ribavirin [11–13], but most of these studies were retrospective, and we do not know whether these substitutions already existed before treatment or were selected by the treatment. A sensitive, real-time polymerase chain reaction (PCR)-based assay for the detection of these mutations in the presence of high levels of wild-type virus is described here. The method is based on the amplification refractory mutation system (ARMS) reverse transcription (RT)-PCR for detection of single base mutations [14,15].

Material and methods

Plasmid DNA controls

Plasmids carrying HCV genotype 1 b core wild-type and mutant clones were made as described previously [16,17] and are summarized in Table I. Plasmid DNA was purified using the QIAprep spin miniprep kit (Qiagen, Hilden, Germany). Plasmids were serially diluted 1:10 in EASY dilution (for real-time PCR) (Takara, Ohtsu, Shiga, Japan) to give a dilution range of 1–1 $\times 10^9$ copies for controls of real-time PCR.

Extraction of HCV-RNA from serum

Serum samples (100 µl) were extracted using the high pure viral RNA kit (Roche Diagnostics, Indianapolis, Ind., USA) according to the manufacturer's protocol. The RNA was eluted in RNase-free water. Written informed consent was obtained from each patient included in this study.

cDNA synthesis and SyBr Green real-time PCR

Reverse transcription was carried out using random hexamers to make HCV cDNA by superscript cDNA synthesis kit (Invitrogen, Carlsbad, Calif., USA). ARMS primers were designed so that the 3′ base matched either the wild-type or mutant sequence [18] (Table II). Each 25-µl reaction contained 2× Power SYBR Green PCR Master Mix (Applied Biosystems, Tokyo, Japan), 2.5 pmol of each primer (Table II). Reactions were run on the Step One real-time PCR system (Applied Biosystems). Cycling conditions were: denaturation at 95°C for 10 min, then 40 cycles at 95°C for 15 s and 60°C for 1 min, followed by a melting curve analysis, confirming their specificity. A plasmid DNA standard was included in each run.

Cloning of clinical HCV sequences and site-directed mutagenesis

To make the plasmid p-core-mutant, PCR products were cloned into pCR-TOPO2.1 vector (Invitrogen). To make the plasmid p-core-wild, PCR-based *in vitro* site-directed mutagenesis was performed using the Quick Change site-directed mutagenesis kit (Stratagene, La Jolla, Calif., USA). DNA sequences of clones were confirmed by direct sequencing.

Results

Optimization of real-time PCR

For this study, real-time PCR using the SYBR Green I detection system (Applied Biosystems) was implemented to detect the HCV amplicon. ARMS PCR specificity is conferred by direct placement of the 3′ end of one of the primers (Figure 1). Cross-reactivity was tested to ensure that the primer sets specifically bound their targets.

When 10^8 copies of the CAA (codon c70) template were amplified using the primer with a base mismatch, approximately 15 cycles were required before the crossing threshold was reached. This compares with 8 cycles for the matching primer. On the other hand, when 10^8 copies of the CGA (codon c70) template were amplified using the primer with a base mismatch, approximately 16 cycles were required before the crossing threshold was reached. This compares with 6 cycles for the matching primer (Figure 1A and B).

When 10^8 copies of the ATG (codon c91) template were amplified using the primer with a base mismatch, approximately 25 cycles were required before the crossing threshold was reached. This compares

Table I. Plasmid DNA used as standard in this study.

Plasmid	Amino acid c70	Codon c70	Amino acid c91	Codon c91
p-core-wild	Arginine	CGA	Leucine	CTG
p-core-mutant	Glutamine	CAA	Methionine	ATG

Table II. Primers used for detection of substitutions at residues c70 (A) and c91 (B).

A.

Primers for detection of substitution at c70		
Primer common to all reactions		
c70 sense primers HCV-c-reverse: 5′-CGGGGTGACAGGAGCCATCC-3′	Codon	Amino acids
HCV 70W: 5′-TATCCCCAAGGCTCGCCG-3′	CGN	Arg
HCV 71M: 5′-TATCCCCAAGGCTCGCCA-3′	CAN	Gln, His

N = A, G, T, or C; Arg = arginine; Gln = glutamine; His = histidine.

B.

Primers for detection of substitution at c91		
Primer common to all reactions		
c91 reverse primers HCV-c-sense: 5′-TCGCAACCTCGTGGAAGGC-3′	Codon	Amino acids
HCV 91W: 5′-CATCCTGCCCACCCCAR-3′	TTG or CTG	Leu
HCV 91M: 5′-CATCCTGCCCACCCCAT-3′	ATG	Met

R = A, G; Met = methionine; Leu = leucine.
HCV sequences are identical to AJ238799. Ref. [11].

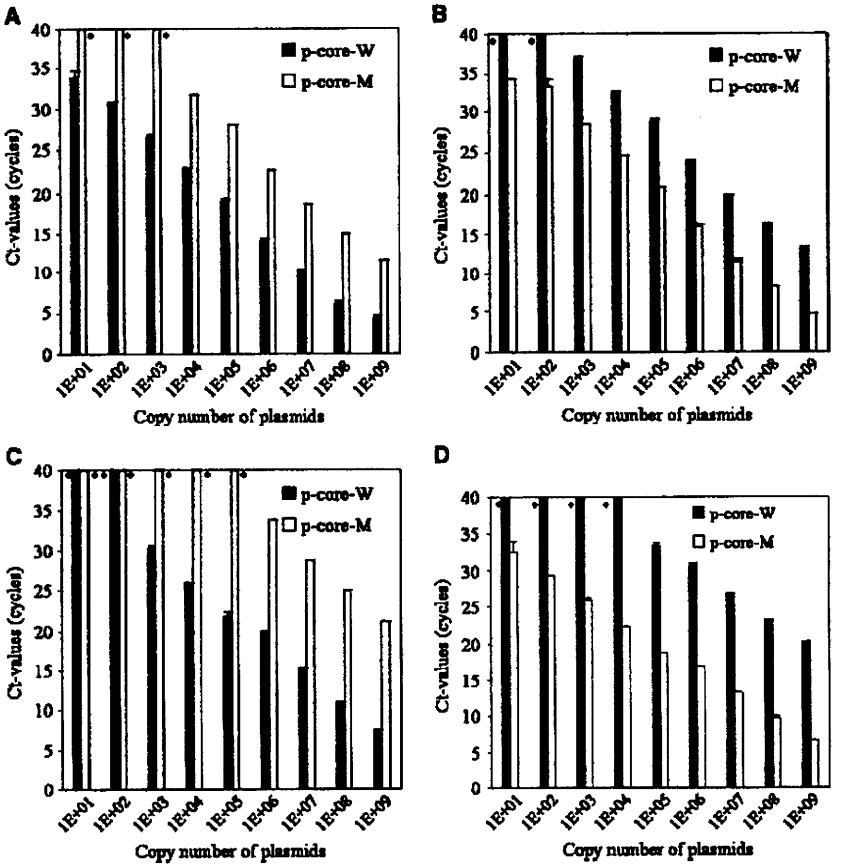

Figure 1. Quantitation of a 10-fold dilution of plasmid p-core-W or p-core-M with wild- or mutant-type primers. Cycle numbers were plotted against the logarithmic concentration of serial dilutions. A. c70-wild primer sets (HCV-70W and HCV-c-reverse). B. c70-mutant primer sets (HCV-70M and HCV-c-reverse). C. c91-wild primer sets (HCV-c-sense and HCV-91W). D. c91-mutant primer sets (HCV-c-sense and HCV-91M). *Unable to detect any signals by 40 cycles.